0013-7227/06/$15.00/0
Printed in U.S.A.

Endocrinology 147(7):3366–3374

doi: 10.1210/en.2006-0216

Osteoblasts Provide a Suitable Microenvironment for the Action of Receptor Activator of Nuclear Factor-κB Ligand

Yohei Yamamoto, Nobuyuki Udagawa, Sachiko Matsuura, Yuko Nakamichi, Hiroshi Horiuchi, Akihiro Hosoya, Midori Nakamura, Hidehiro Ozawa, Kunio Takaoka, Josef M. Penninger, Toshihide Noguchi, and Naoyuki Takahashi

Department of Periodontology (Y.Y., T.N.), School of Dentistry, Aichi-Gakuin University, 464-8650 Aichi, Japan; Department of Biochemistry (Y.Y., N.U., M.N.), Second Department of Anatomy (S.M., A.H.), and Institute for Oral Science (Y.N., H.O., N.T.), Matsumoto Dental University, Nagano 399-0781, Japan; Department of Orthopedic Surgery (H.H.), Shinshu University, School of Medicine, Nagano 390-8621, Japan; Department of Orthopaedic Surgery (K.T.), Osaka City University Graduate School of Medicine, Osaka 545-8585, Japan; and Institute of Molecular Biotechnology of the Austrian Academy of Sciences (J.M.P.), A-1030 Vienna, Austria

Deficiency of osteoprotegerin (OPG), a soluble decoy receptor for receptor activator of nuclear factor-κB ligand (RANKL), in mice induces osteoporosis caused by enhanced bone resorption. Serum concentrations of RANKL are extremely high in OPG-deficient ($OPG^{-/-}$) mice, suggesting that circulating RANKL is involved in osteoclastogenesis. $RANKL^{-/-}$ mice exhibit osteopetrosis, with the absence of osteoclasts. We examined the requirements for osteoclastogenesis using $OPG^{-/-}$ mice, $RANKL^{-/-}$ mice, and a system involving bone morphogenetic protein 2 (BMP-2)-induced ectopic bone formation. When collagen disks containing BMP-2 (BMP-2-disks) or vehicle were implanted into $OPG^{-/-}$ mice, osteoclast-like cells (OCLs) and alkaline phosphatase-positive OCLs appeared in BMP-2-disks but not the control disks. F4/80-positive osteoclast precursors were similarly distributed in both BMP-2- and control disks. Cells expressing RANKL were detected in the BMP-2-disks, and the addition of OPG to the disk inhibited OCL formation. Muscle cells in culture differentiated into alkaline phosphatase-positive cells in the presence of BMP-2 and accordingly expressed RANKL mRNA in response to PTH. This suggests that RANKL expressed by osteoblasts is a requirement for osteoclastogenesis. We then examined how osteoblasts are involved in osteoclastogenesis other than RANKL expression, using $RANKL^{-/-}$ mice. BMP-2- and control disks were implanted into $RANKL^{-/-}$ mice, which were injected with RANKL for 7 d. Many OCLs were observed in the BMP-2-disks and bone tissues but not the control disks. These results suggest that osteoblasts also play important roles in osteoclastogenesis through offering the critical microenvironment for the action of RANKL. (*Endocrinology* 147: 3366–3374, 2006)

OSTEOCLASTS ARE BONE-RESORBING multinucleated cells derived from the monocyte-macrophage lineage (1, 2). Bone-forming osteoblasts express two cytokines essential for osteoclast differentiation: receptor activator of nuclear factor-κB ligand (RANKL) and macrophage colony-stimulating factor (M-CSF) (1–4). Mice deficient for M-CSF (5, 6) or RANKL (7) develop osteopetrosis, with a complete lack of osteoclasts. M-CSF is constitutively expressed by osteoblasts, whereas the expression of RANKL is up-regulated by osteotropic factors such as PTH and 1α,25-dihydroxyvitamin D_3 [1α,25$(OH)_2D_3$] (1–4, 8). Osteoclast precursors bind to RANKL expressed by osteoblasts through cell-cell interaction and differentiate into osteoclasts in the presence of M-CSF (1–4).

Osteoprotegerin (OPG) is a soluble decoy receptor for RANKL (1–4, 9, 10). OPG blocks osteoclastogenesis by inhibiting the RANKL-RANK interaction. Deficiency of OPG in mice results in osteoporosis caused by enhanced bone resorption (11, 12). Serum levels of RANKL are markedly elevated in $OPG^{-/-}$ mice (13). A homozygous deletion of the gene encoding OPG was reported in patients with juvenile Paget's disease, and the serum RANKL level was found to be elevated in one of those patients (14). Recently we demonstrated that circulating RANKL mainly originates from bone in $OPG^{-/-}$ mice (15). These findings suggested that circulating RANKL is involved in osteoclastogenesis in $OPG^{-/-}$ mice. However, it is unclear whether soluble and/or membrane-bound RANKL is the critical trigger for osteoclast formation *in vivo*.

Bone morphogenetic proteins (BMPs) are pluripotent growth factors that have been purified from the bone matrix (16). BMP-2, -4, and -7 can induce ectopic bone formation in animals when they are implanted with appropriate carriers such as type I collagen into sc or muscle tissues (17–20). For instance, BMP-2 inhibits the differentiation of myoblastic

First Published Online April 20, 2006

Abbreviations: ALP, Alkaline phosphatase; BMP, bone morphogenetic protein; GAPDH, glyceraldehyde-3-phosphate dehydrogenase; ITAM, immunoreceptor tyrosine-based activation motifs; M-CSF, macrophage colony-stimulating factor; microCT, microcomputerized tomography; MMP, matrix metalloproteinase; 1α,25$(OH)_2D_3$, 1α,25-dihydroxyvitamin D_3; OPG, osteoprotegerin; OCL, osteoclast-like cell; RANKL, receptor activator of nuclear factor-κB ligand; TRAP, tartrate-resistant acid phosphatase; WT, wild type.

***Endocrinology* is published monthly by The Endocrine Society (http://www.endo-society.org), the foremost professional society serving the endocrine community.**

cells into myotubes and converts their differentiation pathway into the osteoblast lineage (21, 22). However, it is still unclear how osteoclast differentiation is regulated during ectopic bone formation induced by BMPs.

In the present study, we examined the requirements for osteoclastogenesis *in vivo* using OPG$^{-/-}$ mice and a system involving recombinant human BMP-2-induced ectopic bone formation. We also examined the effects of RANKL injection on osteoclast formation in tibiae and BMP-2-induced ectopic bone in RANKL$^{-/-}$ mice. Our results suggest that osteoblasts play important roles in osteoclast formation through offering the critical microenvironment for the action of RANKL as well as RANKL expression.

Materials and Methods

Mice and microcomputerized tomography (microCT)

Male OPG$^{-/-}$ mice (C57BL/6J) and control wild-type (WT) mice were obtained from Japan Clea (Tokyo, Japan). RANKL$^{-/-}$ (C57BL/6) mice were generated in one of the authors' laboratories (7). All procedures for animal care were approved by the Animal Management Committee of Matsumoto Dental University. For microCT analysis, heads and femurs of OPG$^{-/-}$ mice and WT mice were fixed and subjected to three-dimensional microCT analysis.

Ectopic bone formation and tissue preparation

BMP-2 produced by Genetic Institute (Cambridge, MA) was donated to us through Astetellas Pharmaceutical (Tokyo, Japan). BMP-2 containing collagen disks (Helistat; Integra Life Sciences, Plainsboro, NJ) (5 μg/disk) were prepared as described previously (23). In some experiments, OPG-Fc (R&D Systems, Minneapolis, MN) (25 μg/disk) or RANK-Fc (R&D Systems) (25 μg/disk) were added to the BMP-2-containing disks. Collagen disks containing RANKL (PeproTeck, Rocky Hill, NJ) (25 μg/disk) with or without BMP-2 were also prepared. The disks were implanted into the left dorsal muscle pouches of mice (13, 23). After implantation of the disks for 1 or 2 wk, mice were killed to recover the disks with surrounding tissues. Blood samples were also collected from the mice. In some experiments using RANKL$^{-/-}$ mice, the mice were ip injected with RANKL (15 μg/injection) every 2 d for a total of four times. Twenty-four hours after the final RANKL injection, tibiae and implants were removed from the mice for further processing. The implants recovered from mice after implantation for 2 wk were decalcified with EDTA (13, 23). Specimens were embedded in paraffin or Tissue-Tek OCT compound (Sakura Finetechnical, Tokyo, Japan) (24, 25).

Histochemistry

Tartrate-resistant acid phosphatase (TRAP, a marker enzyme of osteoclasts) activity and alkaline phosphatase (ALP, a marker enzyme of osteoblasts) activity in cryostat sections were detected by using enzyme histochemistry as described (13, 25). For double staining of TRAP and ALP, the sections were first incubated for 10 min in an acetate buffer [0.1 M sodium acetate (pH 5.0)] containing naphthol AS-MX phosphate (0.1 mg/ml; Sigma, St. Louis, MO) and fast red violet LB salt (0.6 mg/ml, Sigma) in the presence of 50 mM sodium tartrate to detect TRAP-positive cells. The sections were then washed with PBS and incubated for another 10 min in Tris buffer [0.1 M Tris-HCl (pH 8.5)] containing naphthol AS-MX phosphate (0.1 mg/ml) and fast blue BB salts (0.6 mg/ml, Sigma) to detect ALP-positive cells. TRAP-positive cells appeared as red cells, whereas ALP-positive cells as blue cells. Serial sections were also processed for immunohistochemistry using monoclonal antibody against human cathepsin K (Daiichi Fine Chemical, Takaoka, Japan), polyclonal goat antibodies against mouse matrix metalloproteinase (MMP)-9 (R&D Systems), rat monoclonal antibody against mouse F4/80 (BMA Biomedicals, Augst, Switzerland), and polyclonal goat antibody against mouse RANKL (Santa Cruz Biotechnology, Santa Cruz, CA). The binding of these antibodies to antigens was detected using mouse MOM ABC kit (Vector Laboratories, Burlingame, CA), goat Vectostain ABC kit (Vector Laboratories), or rat Histofine MAX-PO (R) kit, respectively (Nichirei, Tokyo, Japan). Immunocomplexes were visualized with diaminobenzidine (Sigma). The sections were counterstained with hematoxylin.

Measurements of RANKL, OPG, calcium, and TRAP5b levels

Serum concentrations of RANKL and OPG were estimated using respective ELISAs (R&D Systems) (13). Serum calcium concentrations were measured using a calcium E kit (Wako, Tokyo, Japan). Serum TRAP5b activity was measured using a mouse TRAP assay kit (SBA Sciences, Turku, Finland) (26).

Primary muscle cell cultures

Primary muscle cells were prepared from thigh muscles of 1-d-old mice (C57BL/6J) as described previously (22). The primary muscle cells were inoculated at 8×10^4 cells/cm^2 (6-cm culture dish) and cultured with or without 300 ng/ml BMP-2 (R&D Systems). The culture medium was replaced every 2 d. After culturing for 6 d, human PTH (100 ng/ml; R&D Systems) was added to some cultures for 24 h. The cultures were then subjected for double staining of ALP activity and troponin T using antitroponin T monoclonal antibody (Lab Vision, Fremont, CA) (22). Immunoreactions were visualized with a Histofine MAX-PO (R) kit (Nichirei). Some cells were also used for total RNA extraction as described below.

RT-PCR analysis

For RT-PCR analysis, total RNA was extracted from long bones of OPG$^{-/-}$ mice and WT mice using Trizol solution (Invitrogen, Carlsbad, CA). First-strand cDNA was synthesized from the total RNA with random primers and subjected to PCR amplification with Ex Taq polymerase (Takara Biochemicals, Shiga, Japan) using the following specific PCR primers: mouse RANKL, 5′-CGCTCTGTTCCTGTACTTTCGAGCG-3′ (forward, nucleotides 195–219) and 5′-TCGTGCTCCCTCCTTTCATCAGGTT-3 (reverse, nucleotides 757–781); mouse OPG, 5′-TGGAGATCGAATTCTGCTTG-3′ (forward, nucleotides 575–595) and 5′-TCAAGTGCTTGAGGGCATAC-3 (reverse, nucleotides 1275–1295); mouse glyceraldehyde-3-phosphate dehydrogenase (GAPDH), 5′-ACCACAGTCCATGCCATCAC-3′ (forward, nucleotides 566–585) and 5′-TCCACCACCCTGTTGCTGTA-3′ (reverse, nucleotides 998-1017). The PCR products were separated by electrophoresis on 2% agarose gels and visualized by ethidium bromide staining with UV light illumination. The numbers of PCR cycles were: 28 for RANKL and OPG and 20 for GAPDH. The sizes of the PCR products for mouse RANKL, OPG, and GAPDH were 587, 721, and 452 bp, respectively.

Real-time PCR analysis

For real-time PCR analysis, total RNA was extracted from cultures of primary muscle cells. First-strand cDNA was synthesized from total RNA with random primers and subjected to Real-time PCR amplification using the following specific PCR primers: mouse-α1(I) collagen (COL1A1), 5′-TCTCCACTCTTCTAGTTCCT-3′ (forward, nucleotides 1248–1267) and 5′-TTGGGTCATTTCCACATGC-3′ (reverse, nucleotides 1498–1516); mouse RANKL, 5′-TGTACTTTCGAGCGCAGATG-3′ (forward, nucleotides 203–222) and 5′-CCCACAATGTGTTGCAGTTC-3′ (reverse, nucleotides 382–401); and mouse PTH/PTHrP receptor, 5′-AAAGGCCATGCCTACAGACG-3′ (forward, nucleotides 421–440) and 5′-TTCACGAAGATGCTCGCGG-3′ (reverse, nucleotides 701–719). SYBR Green-based quantitative real-time PCR analysis was carried out using the Opticon DNA engine thermocycler (MJ Research, Waltham, MA). Triplicate reactions were carried out for each sample. The expression value of each sample was normalized by the expression level of GAPDH.

Statistics

Data are expressed as the mean ± SD of more than three samples. Statistical analysis was performed using Student's *t* test. Each experiment was repeated at least three times, and similar results were obtained.

Results

Osteoclastogenesis in ectopic bone in OPG$^{-/-}$ mice

MicroCT analysis confirmed that bone mineral content was severely reduced in femurs and alveolar bones obtained from OPG$^{-/-}$ mice at age 18 wk (Fig. 1A). Many TRAP-positive osteoclast-like cells (OCLs) were detected in proximal femurs in OPG$^{-/-}$ mice (Fig. 1A). Although there was no significant difference in serum calcium levels between OPG$^{-/-}$ and WT mice, the serum activity of TRAP5b, a marker of bone resorption, was significantly increased in OPG$^{-/-}$ mice (Fig. 1B). Serum concentrations of RANKL were elevated in OPG$^{-/-}$ mice in comparison with those in WT mice (Fig. 1B). However, RANKL mRNA expression in bone tissues in OPG$^{-/-}$ mice was comparable with that in WT mice (Fig. 1C). These results suggested that circulating RANKL in the serum might be responsible for the increase bone resorption in OPG$^{-/-}$ mice.

We then examined the appearance of OCLs during the ectopic bone formation induced by BMP-2 in OPG$^{-/-}$ and WT mice (Fig. 2). Collagen disks containing BMP-2 or vehicle were implanted into OPG$^{-/-}$ and WT mice, and the implants were recovered after 1 or 2 wk. TRAP-positive cells and ALP-positive cells were observed in BMP-2-disks recovered after 1 wk, preceding the onset of calcification (Fig. 2A). TRAP-positive cells were detected primarily in and around the layers of ALP-positive cells. The number of TRAP-positive cells appearing in BMP-2-disks implanted into OPG$^{-/-}$ mice for 1 wk was markedly higher than that in BMP-2-disks implanted into WT mice (Fig. 2, A and B). Although the mean number of TRAP-positive cells in BMP-2-disks after 2 wk was higher in OPG$^{-/-}$ mice than in WT mice, the significant difference was not recognized between the two BMP-2-disks (Fig. 2B).

Mineralized tissues (bone) were observed in the BMP-2-containing implants recovered after 2 wk. The number of TRAP-positive cells was increased in BMP-2-disks recovered after 2 wk (Fig. 2, A and B). Cells positive for cathepsin K were also observed along the mineralized tissue in the BMP-2-disks (Fig. 2A). Neither TRAP-positive cells nor cathepsin K-positive cells were observed in or around the control disks implanted into OPG$^{-/-}$ mice even after 2 wk (Fig. 2, A and B). Multinucleated OCLs were usually observed in BMP-2-disks recovered after implantation for 2 wk and occasionally in those recovered after 1 wk (Fig. 2C). The multinucleated cells, which appeared in the BMP-2-disks recovered after 1 wk, expressed strong TRAP activity and high levels of the osteoclast-specific proteins cathepsin K and MMP-9 (Fig. 2C). TRAP-positive multinucleated cells were always localized in close contact with ALP-positive cells (Fig. 2C). We previously reported that the serum concentration of RANKL in OPG$^{-/-}$ mice was markedly increased by daily administration of 1α,25(OH)$_2$D$_3$ for 4 d (15). We therefore examined the effect of daily administration of 1α,25(OH)$_2$D$_3$ on the appearance of TRAP-positive cells in the control disks implanted into OPG$^{-/-}$ mice. The effect of 1α,25(OH)$_2$D$_3$ on TRAP-positive cell formation in BMP-2-disks was not examined because there was a possibility that osteoblasts appearing in the BMP-2-disks also expressed RANKL in response to1α,25(OH)$_2$D$_3$. Although the serum concentrations of RANKL in OPG$^{-/-}$ mice were increased to ca 30 ng/ml by 1α,25(OH)$_2$D$_3$ administration, no TRAP-positive cells were detected around or in the control implants (data not shown).

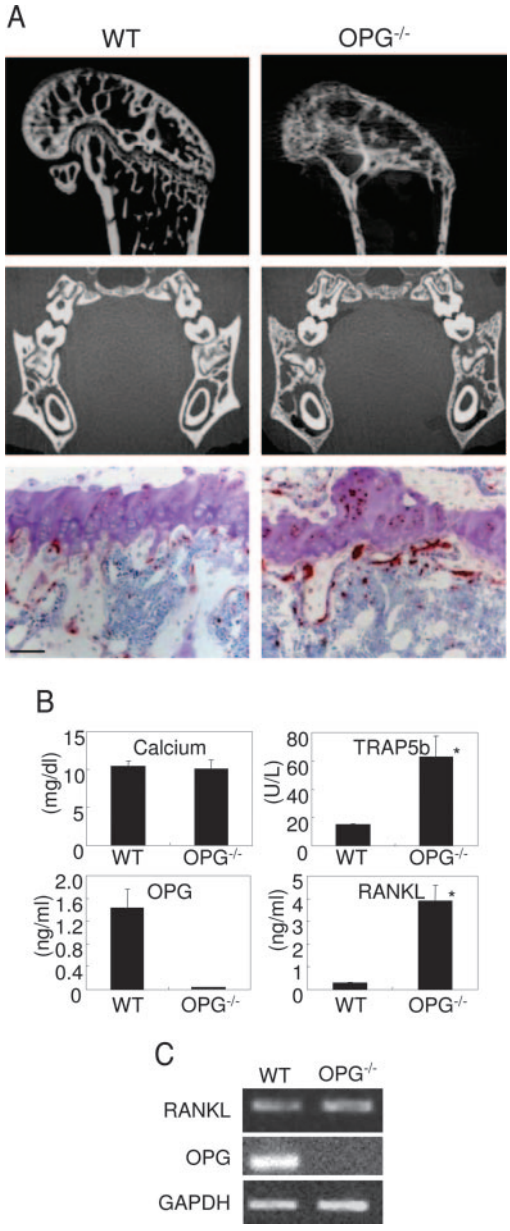

FIG. 1. Features of bone and serum parameters in OPG$^{-/-}$ mice. A, MicroCT images of femurs and alveolar bones in OPG$^{-/-}$ mice and WT mice (*upper panels*). Histological features of the femoral metaphysis in OPG$^{-/-}$ mice and WT mice (*lower panels*) are shown. The relative bone mineral density of femur and mandibular alveolar bone in mice was imaged by microCT. Sections prepared from femurs were histochemically stained for TRAP and then subjected to toluidine blue staining. TRAP-positive cells appear as *red cells*. B, Serum levels of calcium, TRAP5b activity, OPG, and RANKL in OPG$^{-/-}$ mice and WT mice. Serum was collected from OPG$^{-/-}$ mice and WT mice at age 6–8 wk. Concentrations of calcium, OPG, and RANKL in serum were estimated using respective assay kits. Serum TRAP5b activity was estimated using a mouse TRAP assay kit. Data are expressed as the mean ± SD of four animals. *, $P < 0.01$, significantly different from WT mice. C, Expression of RANKL and OPG mRNAs in bone tissues in OPG$^{-/-}$ mice and WT mice. Total RNA was extracted from long bones and subjected to RT-PCR analysis for RANKL and OPG mRNAs.

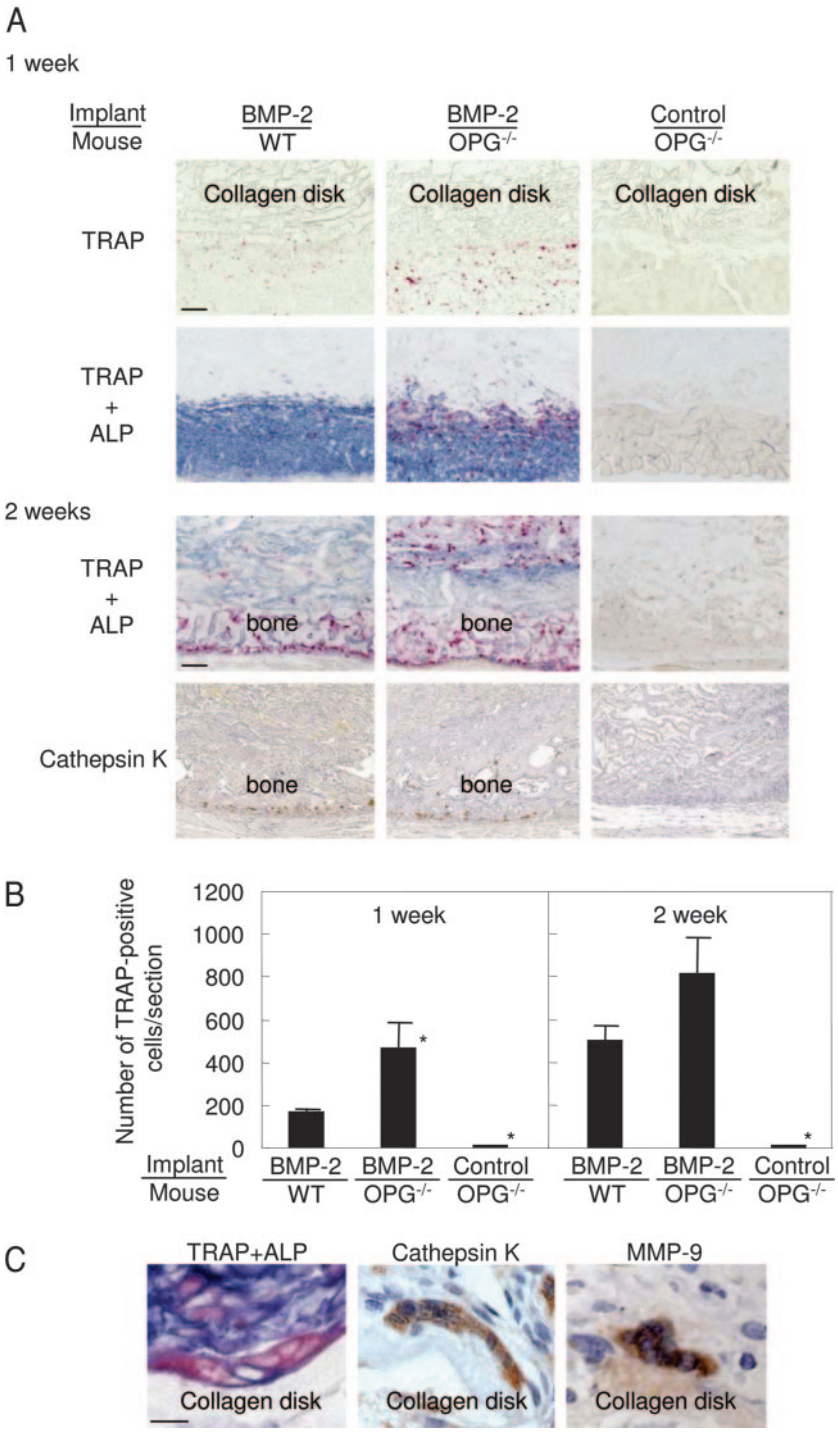

FIG. 2. Expression of specific markers of osteoclasts and osteoblasts in implants containing BMP-2 or vehicle. Collagen disks containing BMP-2 or vehicle (control) were implanted into $OPG^{-/-}$ mice and WT mice and recovered after implantation for 1 or 2 wk. A, Sections were prepared from the implants and histochemically stained for TRAP and double stained for TRAP and ALP. TRAP-positive cells appeared as *red cells* and ALP-positive cells as *blue cells*. Sections prepared from the implants recovered after 2 wk were immunohistochemically stained for cathepsin K and then subjected to hematoxylin staining. Cathepsin K-positive cells stained brown. *Bar*, 100 μm. B, The number of TRAP-positive cells was counted in each section. Data are expressed as the mean ± SD from three implants. *, $P < 0.05$, significantly different from WT mice. C, Histochemical observation of multinucleated cells. BMP-2-disks implanted into $OPG^{-/-}$ mice were recovered after implantation for 1 wk. Sections were double stained for TRAP and ALP. Some sections were also immunohistochemically stained for cathepsin K and MMP-9 (*brown color*) and subjected to hematoxylin staining. *Bar*, 10 μm.

Inhibition of OCL formation by OPG-Fc or RANK-Fc

We next examined whether RANKL is involved in the appearance of OCLs in the BMP-2-disks. Collagen disks containing BMP-2 together with OPG-Fc or RANK-Fc were implanted into $OPG^{-/-}$ mice for 1 wk. Both OPG-Fc and RANK-Fc have been shown to inhibit osteoclastogenesis through inhibiting the interaction between RANKL and RANK. Although TRAP-positive multinucleated cells were hardly observed in BMP-2-disks recovered after implantation for 1 wk, many TRAP-positive mononuclear cells were induced in the disks (Fig. 3A). The addition of OPG-Fc to the BMP-2-disks almost completely inhibited the appearance of TRAP-positive cells (Fig. 3, A and B). TRAP-positive cell formation was strongly inhibited by RANK-Fc as well. Neither OPG-Fc nor RANK-Fc affected the number of ALP-positive cells appearing in BMP-2-disks. The number of MMP-9-positive cells in BMP-2-disks was also reduced by OPG-Fc (Fig. 3B). We previously reported that F4/80-positive macro-

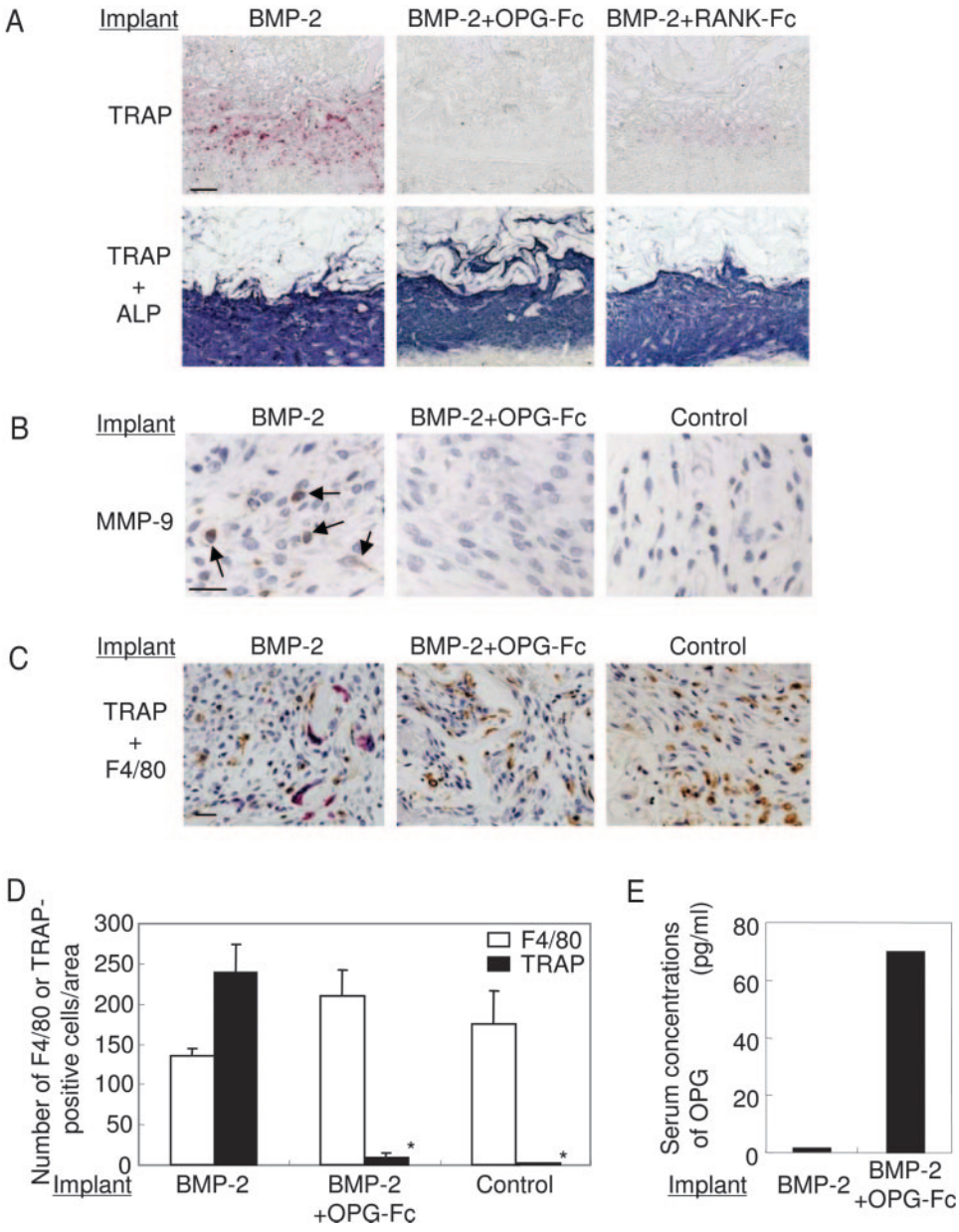

FIG. 3. Effects of OPG-Fc and RANK-Fc on the appearance of OCLs and ALP-positive cells in implants containing BMP-2. Collagen disks containing BMP-2, BMP-2 plus OPG (BMP-2 + OPG-Fc), or BMP-2 plus soluble RANK (BMP-2 + RANK-Fc) were prepared and implanted into $OPG^{-/-}$ mice. The implants were recovered after implantation for 1 wk. A, Histochemical detection of TRAP- and ALP-positive cells in the implants. Sections were histochemically stained for TRAP and double stained for TRAP and ALP. *Bar*, 100 μm. B, Immunohistochemical detection of MMP-9-positive cells in the implants. Collagen disks containing BMP-2, BMP-2 plus OPG-Fc (BMP-2 + OPG-Fc), or vehicle (control) were implanted into $OPG^{-/-}$ mice. The implants were recovered after implantation for 1 wk. *Bar*, 20 μm. C, D, and E, Collagen disks containing BMP-2, BMP-2 plus OPG-Fc (BMP-2 + OPG-Fc), or vehicle (control) were implanted into $OPG^{-/-}$ mice. C, Sections prepared from the implants were double stained for TRAP and F4/80. *Bar*, 20 μm. D, The number of F4/80-positive cells and that of TRAP-positive cells per unit area (1.0 mm^2) were separately counted. Data are expressed as the mean ± SD of three implants. *, $P < 0.01$, significantly different from implants containing BMP-2 alone. E, Serum concentrations of OPG in $OPG^{-/-}$ mice implanted with collagen disks containing BMP-2 and BMP-2 together with OPG-Fc (BMP-2 + OPG-Fc). The serum of mice in each group was combined, and the concentration of OPG in the serum was measured by ELISA.

phages differentiated into OCLs in the presence of RANKL and M-CSF (23). There was no significant difference in the distribution of F4/80-positive cells between BMP-2-disks and control ones (Fig. 3, C and D). TRAP-positive cells were observed only in the BMP-2-disks. The addition of OPG-Fc to BMP-2-containing disks had no effect on the appearance of F4/80-positive cells but strongly inhibited the appearance of TRAP-positive cells (Fig. 3, C and D). OPG-Fc that had leaked from the disks was detected in the serum of $OPG^{-/-}$ mice (Fig. 3E). Thus, OPG inhibited the appearance of OCLs but not OCL progenitor cells in the implants.

Importance of RANKL expressed by BMP-2-induced ALP-positive cells in osteoclastogenesis

Cells expressing RANKL were detected immunohistochemically in and around the BMP-2-disks but not control disks (Fig. 4). The addition of OPG-Fc to the BMP-2-disk had no effect on the expression of RANKL protein by stromal cells (Fig. 4A). This suggests that locally expressed RANKL is important for the induction of OCLs in BMP-2-induced ectopic bone. We then examined whether BMP-2 directly induces RANKL expression in myoblastic cells (Fig. 4B). Primary muscle cells prepared from thigh muscles of newborn mice were cultured in the presence or absence of BMP-2 for 6 d (22). The number of troponin T (a marker of myotubes)-positive myotubes was decreased and that of ALP-positive cells was increased in muscle cell cultures treated with BMP-2 (Fig. 4B). Real-time PCR analysis showed that primary muscle cells treated with recombinant human BMP-2 expressed mRNAs of α1(I)-collagen and PTH/PTHrP receptors but not RANKL (Fig. 4C). RANKL mRNA was expressed in BMP-2-treated cells when they were further incubated with

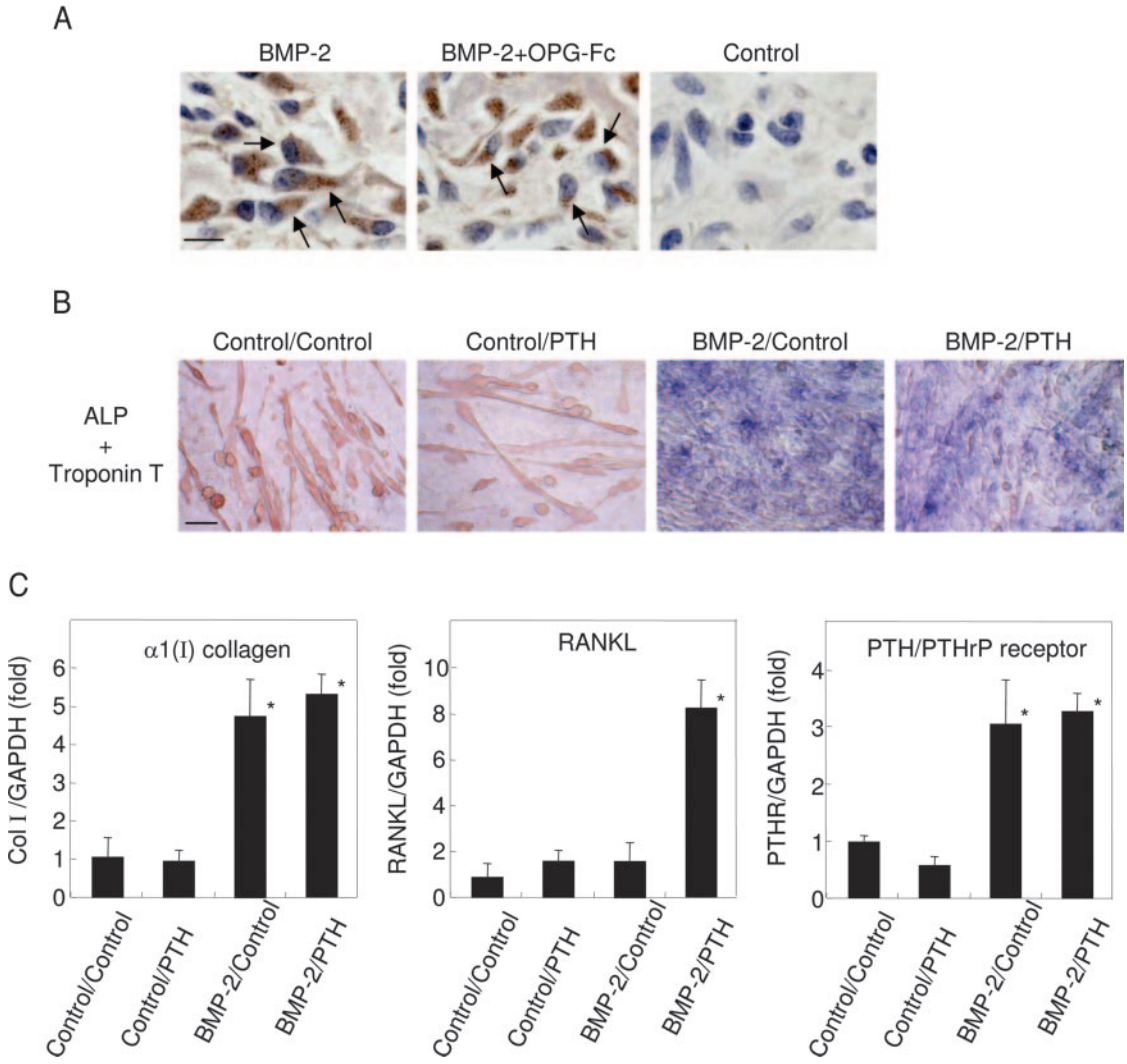

FIG. 4. Expression of RANKL in ALP-positive cells induced by BMP-2. A, Expression of RANKL protein in ALP-positive cells induced by in implants containing BMP-2 or vehicle. Collagen disks containing BMP-2, BMP-2 plus OPG-Fc (BMP-2 + OPG-Fc), or vehicle (control) were implanted into $OPG^{-/-}$ mice and recovered after implantation for 1 wk. Sections of the implants were immunohistochemically stained for RANKL using anti-RANKL antibody and subjected to hematoxylin staining. RANKL-positive cells appeared as *brown cells* (*arrows*). Bar, 10 μm. B and C, Effects of BMP-2 and PTH on RANKL mRNA expression in primary muscle cells in culture. Primary muscle cells were cultured in the presence or absence of BMP-2 for 6 d and further incubated with or without PTH for 24 h (control/control, control/PTH, BMP-2/control, BMP-2/PTH). Subsequently cells were stained for both ALP and troponin T. Some cultures were subjected to extraction of total RNA. B, Double staining of muscle cell cultures for ALP activity and troponin T. Troponin T-positive cells appeared as *red cells* and ALP-positive cells as *blue cells*. *Bar*, 50 μm. C, Real-time RT-PCR for mRNAs of α1(I) collagen, PTH/PTHrP receptors, and RANKL. The expression of α1(I) collagen, PTH/PTHrP receptor, and RANKL mRNA was expressed as fold increase relative to GAPDH expression. Data are expressed as the mean ± SD of three cultures. *, $P < 0.01$, significantly different from control/control cultures.

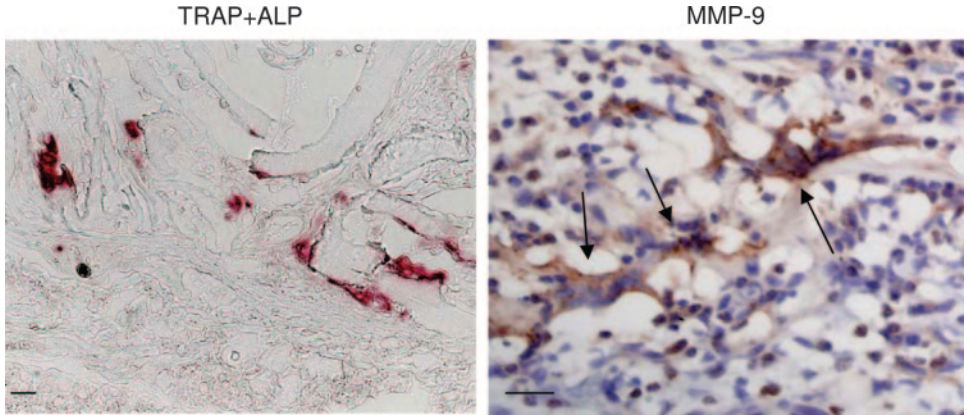

FIG. 5. Expression of specific markers of osteoclasts in implants containing RANKL. Collagen disks containing RANKL (25 μg/disk) were implanted into $OPG^{-/-}$ mice. The implants were recovered after implantation for 1 wk. Sections were double stained for TRAP and ALP (*left panel*). Sections were also immunohistochemically stained for MMP-9 and then subjected to hematoxylin staining (*right panel*). *Arrows* indicate MMP-9-positive cells. The number of TRAP-positive cells was counted in each section (22.8 ± 7.4 TRAP-positive cells per section, the mean ± SD of five sections). *Bar*, 20 μm.

PTH (Fig. 4C). These results suggest that BMP-2 induces the differentiation of myoblasts into osteoblasts, which express RANKL in response to osteotropic factors, including PTH.

We next examined whether collagen disks containing RANKL but not BMP-2 induced OCLs in the disks (Fig. 5). Collagen disks containing RANKL (25 μg/disk) were implanted into OPG$^{-/-}$ mice for 1 wk. TRAP-positive cells appeared in the disks, although the number was very low (22.8 ± 7.4 TRAP-positive cells per section, the mean ± SD of five sections). ALP-positive cells were not observed in the disks. A small number of MMP-9-positive cells were also observed in the RANKL-containing disks. These results suggest that RANKL is involved in OCL formation in the collagen disks and further confirm that OCL precursors are present in the control disks as well as the BMP-2-disks.

Osteoblasts determine the site of osteoclastogenesis

We finally examined the role of osteoblasts in osteoclastogenesis using RANKL$^{-/-}$ mice (Fig. 6). BMP-2-disks and control disks were implanted into RANKL$^{-/-}$ mice. After implantation for 1 wk, RANKL (15 μg/injection) was injected into RANKL$^{-/-}$ mice every 2 d for a total of four times. Osteoclasts were totally absent in tibiae of RANKL$^{-/-}$ mice (Fig. 6A). Injection of RANKL into RANKL$^{-/-}$ mice induced many TRAP-positive cells in the tibiae as if they were existing in WT mice. TRAP-positive cells were never observed in soft tissues around the bones in RANKL$^{-/-}$ mice injected with RANKL (Fig. 6A). ALP-positive cells appeared in BMP-2-disks implanted into RANKL$^{-/-}$ mice, but TRAP-positive cells did not (Fig. 6B). Many TRAP-positive cells were also detected in the BMP-2-disks implanted into RANKL$^{-/-}$ mice injected with RANKL, whereas only a few TRAP-positive cells were observed in the control disks. Most TRAP-positive cells were localized in close proximity to ALP-positive cells. These results suggest that osteoblasts play critical roles in osteoclastogenesis, even under conditions of high levels of circulating RANKL, and that circulating RANKL in the serum is also involved in the increase bone resorption in OPG$^{-/-}$ mice.

Discussion

OPG$^{-/-}$ mice exhibit aberrant bone metabolism characterized by accelerated bone resorption (11–13). Because the serum concentration of RANKL is markedly elevated in these mice (15), we hypothesized that if circulating RANKL is directly involved in osteoclastogenesis, osteoclasts would be

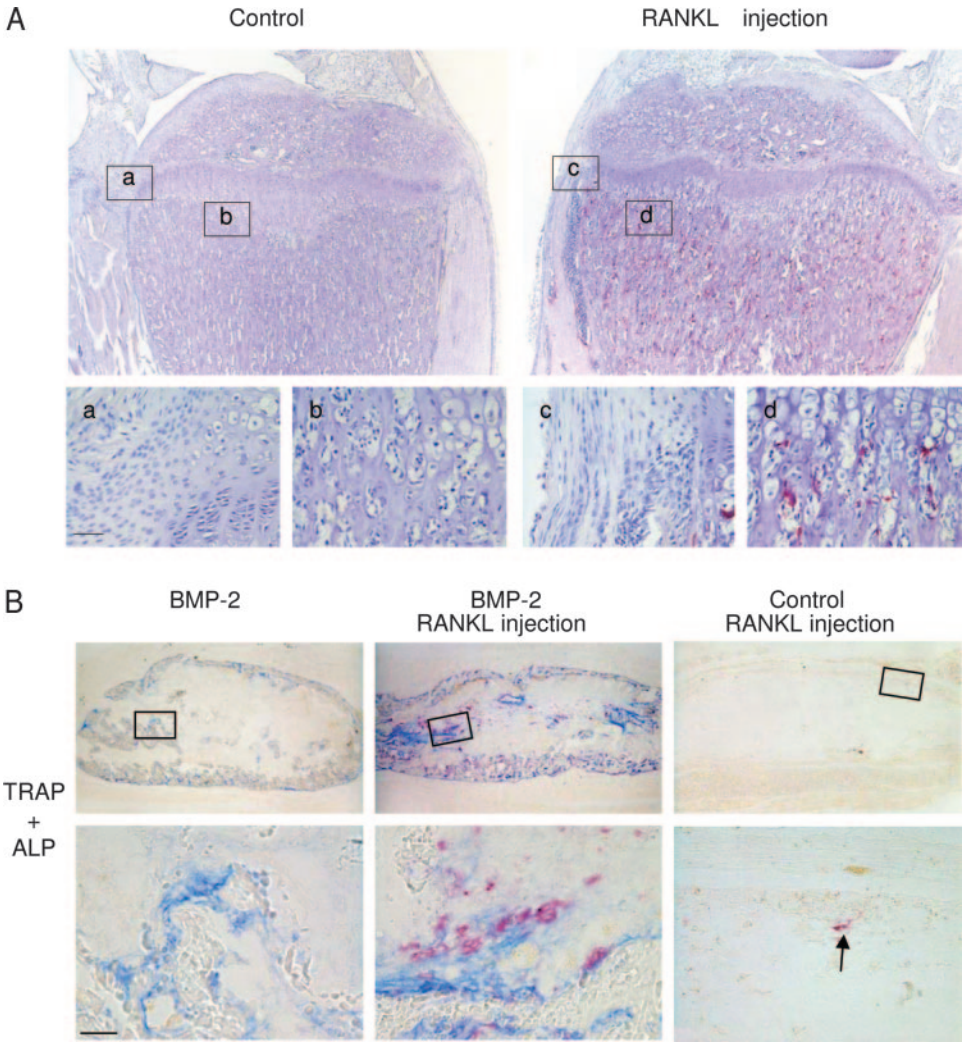

FIG. 6. Effects of RANKL injection on BMP-2-mediated osteoclast formation in RANKL$^{-/-}$ mice. Collagen disks containing BMP-2 or vehicle (control) were implanted into RANKL$^{-/-}$ mice. After implantation for 1 wk, mice were ip injected with RANKL (15 μg/head per day) every 2 d for a total of four times. Twenty-four hours after the final injection, tibiae and implants were removed from the mice. A, Sections of tibiae were histochemically stained for TRAP and then subjected to hematoxylin staining. a–d, High-power views of the portions in squares in the *upper panels*. B, Sections of implants were double stained for TRAP and ALP. TRAP-positive cells appeared as *red cells* and ALP-positive cells as *blue cells*. *Lower panels* show high-power views of the portions in squares in the *upper panels*. The *arrow* indicates a TRAP-positive cell found in a control disk. *Bars*, 50 μm.

induced in tissues other than bone in these mice. However, our experiments showed that only ALP-positive osteoblast-like cells, but not serum RANKL, supported OCL formation in $OPG^{-/-}$ mice. TRAP-positive cells were always detected in and around the layers of ALP-positive cells in BMP-2-disks but not the control disks. TRAP-positive cells also expressed osteoclast markers such as cathepsin K and MMP-9, confirming the notion that these cells were bona fide OCLs. TRAP-positive cells and MMP-9-positive cells did not develop in BMP-2-disks containing OPG-Fc or RANK-Fc. These results show that osteoblasts support OCL formation in BMP-containing disks.

We showed that the ALP-positive cells appearing in the BMP-2-disks expressed RANKL protein. BMP-2 induced the differentiation of muscle cells into ALP-positive cells, which then expressed RANKL mRNA in response to PTH. It was reported that treatment of myoblastic C2C12 cells with BMP-2-induced RANKL mRNA expression in the presence of $1\alpha,25(OH)_2D_3$ (27). These results suggest that BMP-2 converts the differentiation pathway of myoblasts into a pathway generating osteoblasts responsive to calcitropic hormones such as PTH and $1\alpha,25(OH)_2D_3$. TGFβ has been reported to enhance osteoclast formation in cultures of osteoclast progenitor cells treated with RANKL (28–30). These results suggest that cytokines such as TGFβ and M-CSF in addition to RANKL are involved in OCL formation in BMP-2-disks. Osteoblasts and several cytokines induced by BMP-2 appear to play important roles in OCL formation in BMP-2-induced ectopic bone tissues.

Mineralized tissues are not required for osteoclast differentiation, even under *in vivo* conditions. Irie *et al.* (24) examined osteoclast formation during BMP-2-induced ectopic bone formation. ALP-positive cells and mononuclear cells possessing osteoclast markers such as TRAP, cathepsin K, and calcitonin receptors simultaneously appeared on d 3 after implantation of the BMP-2-containing substrate in rats (24). These results, together with our findings, suggest that osteoblasts rather than mineralized tissues determine the site at which osteoclasts develop through local expression of RANKL at the site.

F4/80-positive cells were similarly distributed in the control disks and BMP-2-containing disks. We previously reported that bone marrow-derived F4/80-positive macrophages effectively differentiated into OCLs in the presence of RANKL and M-CSF (31). Circulating monocytes seem to differentiate into F4/80-positive macrophages in the connective tissues induced by both the BMP disks and control disks. RT-PCR analysis showed that the connective tissue in the control implants expressed M-CSF mRNA (data not shown), suggesting that the connective tissue in the implant supplies M-CSF. In fact, OCLs appeared in RANKL-containing collagen disks, although the number was very low. These results suggest that osteoclast precursors are present, even in the control disks, and that the expression of M-CSF is not the determining factor for osteoclast formation in BMP-2-disks.

Interestingly, injection of RANKL into $RANKL^{-/-}$ mice induced many TRAP-positive cells on the surface of calcified bone tissues but not in soft tissues around the bone. In addition, OCLs were induced in BMP-2-disks, and they were observed in and around the layers of ALP-positive cells. These results suggest that, in addition to RANKL expression, osteoblasts play important roles in osteoclast formation. We previously reported that membrane- or matrix-associated forms of M-CSF expressed by osteoblasts supported osteoclast formation in cocultures with osteoclast progenitors (32). The distribution of membrane- or matrix-associated forms of M-CSF may determine the site of osteoclast formation. Recent studies have shown that RANKL and M-CSF are not sufficient to activate the signals required for osteoclastogenesis and that immunoreceptor tyrosine-based activation motifs (ITAM)-dependent costimulatory signals are also required to induce osteoclastogenesis (33–36). ITAM-dependent costimulatory signals may be involved in inducing osteoclastogenesis in the correct place. Alternatively, osteoblasts may express important signal(s) other than M-CSF, RANKL, and ligands that stimulate ITAM signals that determine where osteoclastogenesis can occur. Alternatively, osteoblasts may express an unidentified signal(s) to determine the correct location for osteoclastogenesis. These results also suggest that circulating RANKL in the serum is involved in the increase bone resorption in $OPG^{-/-}$ mice.

Soluble RANKL is sufficient in inducing *in vitro* osteoclastogenesis in the absence of osteoblasts (5, 7). When collagen disks containing RANKL were implanted into $OPG^{-/-}$ mice for 1 wk, TRAP-positive cells appeared in the disks. However, the number of TRAP-positive cells was very low in the control disks containing RANKL in comparison with that in BMP-2-containing disks. These results suggest that osteoblasts offer the critical microenvironment for the action of RANKL. The amount of RANKL necessary for osteoclastogenesis may lower in the presence of osteoblasts. Osteoclasts or OCLs are also detected in soft tissues such as giant cell tumors (37–39) and the synovium of the inflamed joints in rheumatoid arthritis patients (40, 41). Because osteoblasts are not observed in those soft tissues, stromal cells in such tissues may pay a role similar to that of osteoblasts in osteoclast formation.

In conclusion, osteoblasts play important roles to induce osteoclasts in suitable sites. Osteoblasts express RANKL and M-CSF, two cytokines essential for osteoclast formation. In addition, osteoblasts provide the critical microenvironment for the action of RANKL to induce osteoclasts. Further studies will elucidate the molecular mechanism by which sites of osteoclastogenesis are selected and developed.

Acknowledgments

Received February 17, 2006. Accepted April 11, 2006.

Address all correspondence and requests for reprints to: Nobuyuki Udagawa, Department of Biochemistry, Matsumoto Dental University, 1780 Gobara, Hiro-oka, Shiojiri, Nagano 399-0781, Japan. E-mail: udagawa@po.mdu.ac.jp.

This work was supported in part by Grants-in-Aid 12137209, 16390535, 16659578, 15390641, and 15659445 and Aichi Gakuin University (AGU) High-Tech Research Center Project from the Ministry of Education, Culture, Sports, Science, and Technology of Japan. This study is carried out as a part of Ground-based Research Announcement for Space Utilization promoted by Japan Space Forum.

Disclosure: The authors (Y.Y., N.U., S.M., Y.N., H.H., A.H., M.N., H.O., K.T., J.M.P., T.N., and N.T.) have no conflicting financial interests, and have nothing to declare.

References

1. **Suda T, Takahashi N, Udagawa N, Jimi E, Gillespie MT, Martin TJ** 1999 Modulation of osteoclast differentiation and function by the new members of the tumor necrosis factor receptor and ligand families. Endocr Rev 20:345–357
2. **Teitelbaum SL** 2000 Osteoclasts, integrins, and osteoporosis. J Bone Miner Metab 18:344–349
3. **Boyle WJ, Simonet WS, Lacey DL** 2003 Osteoclast differentiation and activation. Nature 15:337–342
4. **Arron JR, Choi Y** 2000 Bone versus immune system. Nature 408:535–536
5. **Yoshida H, Hayashi S, Kunisada T, Ogawa M, Nishikawa S, Okamura H, Sudo T, Shultz LD, Nishikawa S** 1990 The murine mutation osteopetrosis is in the coding region of the macrophage colony stimulating factor gene. Nature 345:442–444
6. **Wiktor-Jedrzejczak W, Bartocci A, Ferrante Jr AW, Ahmed-Ansari A, Sell KW, Pollard JW, Stanley ER** 1990 Total absence of colony-stimulating factor 1 in the macrophage-deficient osteopetrotic (op/op) mouse. Proc Natl Acad Sci USA 87:4828–4832
7. **Kong YY, Yoshida H, Sarosi I, Tan HL, Timms E, Capparelli C, Morony S, Oliveira-dos-Santos AJ, Van G, Itie A, Khoo W, Wakeham A, Dunstan CR, Lacey DL, Mak TW, Boyle WJ, Penninger JM** 1999 OPGL is a key regulator of osteoclastogenesis, lymphocyte development and lymph-node organogenesis. Nature 397:315–323
8. **Yasuda H, Shima N, Nakagawa N, Yamaguchi K, Kinosaki M, Mochizuki S, Tomoyasu A, Yano K, Goto M, Murakami A, Tsuda E, Morinaga T, Higashio K, Udagawa N, Takahashi N, Suda T** 1998 Osteoclast differentiation factor is a ligand for osteoprotegerin/osteoclastogenesis-inhibitory factor and is identical with TRANCE/RANKL. Proc Natl Acad Sci USA 95:3597–3602
9. **Simonet WS, Lacey DL, Dunstan CR, Kelley M, Chang MS, Luthy R, Nguyen HQ, Wooden S, Bennett L, Boone T, Shimamoto G, DeRose M, Elliott R, Colombero A, Tan HL, Trail G, Sullivan J, Davy E, Bucay N, Renshaw-Gegg L, Hughes TM, Hill D, Pattison W, Campbell P, Sander S, Van G, Tarpley J, Derby P, Lee R, Boyle WJ** 1997 Osteoprotegerin: a novel secreted protein involved in the regulation of bone density. Cell 89:309–319
10. **Yasuda H, Shima N, Nakagawa N, Mochizuki SI, Yano K, Fujise N, Sato Y, Goto M, Yamaguchi K, Kuriyama M, Kanno T, Murakami A, Tsuda E, Morinaga T, Higashio K** 1998 Identity of osteoclastogenesis inhibitory factor (OCIF) and osteoprotegerin (OPG): a mechanism by which OPG/OCIF inhibits osteoclastogenesis *in vitro*. Endocrinology 139:1329–1337
11. **Bucay N, Sarosi I, Dunstan CR, Morony S, Tarpley J, Capparelli C, Scully S, Tan HL, Xu W, Lacey DL, Boyle WJ, Simonet WS** 1998 Osteoprotegerin-deficient mice develop early onset osteoporosis and arterial calcification. Genes Dev 12:1260–1268
12. **Mizuno A, Amizuka N, Irie K, Murakami A, Fujise N, Kanno T, Sato Y, Nakagawa N, Yasuda H, Mochizuki S, Gomibuchi T, Yano K, Shima N, Washida N, Tsuda E, Morinaga T, Higashino K, Ozawa H** 1998 Severe osteoporosis in mice lacking osteoclastogenesis inhibitory factor/osteoprotegerin. Biochem Biophys Res Commun 247:610–615
13. **Nakamura M, Udagawa N, Matsuura S, Mogi M, Nakamura H, Horiuchi H, Saito N, Hiraoka BY, Kobayashi Y, Takaoka K, Ozawa H, Miyazawa H, Takahashi N** 2003 Osteoprotegerin regulates bone formation through a coupling mechanism with bone resorption. Endocrinology 144:5441–5449
14. **Whyte MP, Obrecht SE, Finnegan PM, Jones JL, Podgornik MN, McAlister WH, Mumm S** 2002 Osteoprotegerin deficiency and juvenile Paget's disease. N Engl J Med 347:175–184
15. **Nakamichi Y, Udagawa N, Nakamura M, Kobayashi Y, Mogi M, Takahashi N** 2004 Osteoprotegerin tightly regulates the shedding of RANKL by osteoblast and activated T cells J Bone Miner Res 19:S50
16. **Wozney JM, Rosen V, Celeste AJ, Mitsock LM, Whitters MJ, Kriz RW, Hewick RM, Wang EA** 1988 Novel regulators of bone formation: molecular clones and activities. Science 242:1528–1534
17. **Yamaguchi A, Komori T, Suda T** 2000 Regulation of osteoblast differentiation mediated by bone morphogenetic proteins, hedgehogs, and Cbfa1. Endocr Rev 21:393–411
18. **Canalis E, Economides AN, Gazzerro E** 2003 Bone morphogenetic proteins, their antagonists, and the skeleton. Endocr Rev 24:218–235
19. **Waite KA, Eng C** 2003 From developmental disorder to heritable cancer: it's all in the BMP/TGFβ family. Nat Rev Genet 4:763–773
20. **Shimasaki S, Moore RK, Otsuka F, Erickson GF** 2004 The bone morphogenetic protein system in mammalian reproduction. Endocr Rev 25:72–101
21. **Yamaguchi A, Katagiri T, Ikeda T, Wozney JM, Rosen V, Wang EA, Kahn AJ, Suda T, Yoshiki S** 1991 Recombinant human bone morphogenetic protein-2 stimulates osteoblastic maturation and inhibits myogenic differentiation *in vitro*. J Cell Biol 113:681–687
22. **Katagiri T, Yamaguchi A, Komaki M, Abe E, Takahashi N, Ikeda T, Rosen V, Wozney JM, Fujisawa-Sehara A, Suda T** 1994 Bone morphogenetic protein-2 converts the differentiation pathway of C2C12 myoblasts into the osteoblast lineage. J Cell Biol 127:1755–1766
23. **Horiuchi H, Saito N, Kinoshita T, Wakabayashi S, Tsutsumimoto T, Takaoka K** 2001 Enhancement of bone morphogenetic protein-2-induced new bone formation in mice by the phosphodiesterase inhibitor pentoxifylline. Bone 28:290–294
24. **Irie K, Alpaslan C, Takahashi K, Kondo Y, Izumi N, Sakakura Y, Tsuruga E, Nakajima T, Ejiri S, Ozawa H, Yajima T** 2003 Osteoclast differentiation in ectopic bone formation induced by recombinant human bone morphogenetic protein 2 (rhBMP-2). J Bone Miner Metab 21:363–369
25. **Sato N, Takahashi N, Suda K, Nakamura M, Yamaki M, Ninomiya T, Kobayashi Y, Takada H, Shibata K, Yamamoto M, Takeda K, Akira S, Noguchi T, Udagawa N** 2004 MyD88 but not TRIF is essential for osteoclastogenesis induced by lipopolysaccharide, diacyl lipopeptide, and IL-1α. J Exp Med 200:601–611
26. **Halleen JM, Alatalo SL, Suominen H, Cheng S, Janckila AJ, Vaananen HK** 2000 Tartrate-resistant acid phosphatase 5b: a novel serum marker of bone resorption. J Bone Miner Res 15:1337–1345
27. **Otsuka E, Notoya M, Hagiwara H** 2003 Treatment of myoblastic C2C12 cells with BMP-2 stimulates vitamin D-induced formation of osteoclasts. Calcif Tissue Int 73:72–77
28. **Sells Galvin RJ, Gatlin CL, Horn JW, Fuson TR** 1999 TGF-β enhances osteoclast differentiation in hematopoietic cell cultures stimulated with RANKL and M-CSF. Biochem Biophys Res Commun 265:233–239
29. **Massey HM, Scopes J, Horton MA, Flanagan AM** 2001 Transforming growth factor-β1 (TGF-β) stimulates the osteoclast-forming potential of peripheral blood hematopoietic precursors in a lymphocyte-rich microenvironment. Bone 28:577–582
30. **Fox SW, Haque SJ, Lovibond AC, Chambers TJ** 2003 The possible role of TGF-β-induced suppressors of cytokine signaling expression in osteoclast/macrophage lineage commitment *in vitro*. J Immunol 170:3679–3687
31. **Kobayashi K, Takahashi N, Jimi E, Udagawa N, Takami M, Kotake S, Nakagawa N, Kinosaki M, Yamaguchi K, Shima N, Yasuda H, Morinaga T, Higashio K, Martin TJ, Suda T** 2000 Tumor necrosis factor α stimulates osteoclast differentiation by a mechanism independent of the ODF/RANKL-RANK interaction. J Exp Med 191:275–286
32. **Itoh K, Udagawa N, Matsuzaki K, Takami M, Amano H, Shinki T, Ueno Y, Takahashi N, Suda T** 2000 Importance of membrane- or matrix-associated forms of M-CSF and RANKL/ODF in osteoclastogenesis supported by SaOS-4/3 cells expressing recombinant PTH/PTHrP receptors. J Bone Miner Res 15:1766–1775
33. **Kaifu T, Nakahara J, Inui M, Mishima K, Momiyama T, Kaji M, Sugahara A, Koito H, Ujike-Asai A, Nakamura A, Kanazawa K, Tan-Takeuchi K, Iwasaki K, Yokoyama WM, Kudo A, Fujiwara M, Asou H, Takai T** 2003 Osteopetrosis and thalamic hypomyelinosis with synaptic degeneration in DAP12-deficient mice. J Clin Invest 111:323–332
34. **Koga T, Inui M, Inoue K, Kim S, Suematsu A, Kobayashi E, Iwata T, Ohnishi H, Matozaki T, Kodama T, Taniguchi T, Takayanagi H, Takai T** 2004 Costimulatory signals mediated by the ITAM motif cooperate with RANKL for bone homeostasis. Nature 428:758–763
35. **Mocsai A, Humphrey MB, Van Ziffle JA, Hu Y, Burghardt A, Spusta SC, Majumdar S, Lanier LL, Lowell CA, Nakamura MC** 2004 The immunomodulatory adapter proteins DAP12 and Fc receptor γ-chain (FcRγ) regulate development of functional osteoclasts through the Syk tyrosine kinase. Proc Natl Acad Sci USA 101:6158–6163
36. **Kim N, Takami M, Rho J, Josien R, Choi Y** 2002 A novel member of the leukocyte receptor complex regulates osteoclast differentiation. J Exp Med 195:201–209
37. **Kartsogiannis V, Zhou H, Horwood NJ, Thomas RJ, Hards DK, Quinn JM, Niforas P, Ng KW, Martin TJ, Gillespie MT** 1999 Localization of RANKL (receptor activator of NF κB ligand) mRNA and protein in skeletal and extraskeletal tissues. Bone 25:525–534
38. **Morgan T, Atkins GJ, Trivett MK, Johnson SA, Kansara M, Schlicht SL, Slavin JL, Simmons P, Dickinson I, Powell G, Choong PF, Holloway AJ, Thomas DM** 2005 Molecular profiling of giant cell tumor of bone and the osteoclastic localization of ligand for receptor activator of nuclear factor κB. Am J Pathol 167:117–128
39. **Lau YS, Sabokbar A, Gibbons CL, Giele H, Athanasou N** 2005 Phenotypic and molecular studies of giant-cell tumors of bone and soft tissue. Hum Pathol 36:945–954
40. **Gravallese EM, Manning C, Tsay A, Naito A, Pan C, Amento E, Goldring SR** 2000 Synovial tissue in rheumatoid arthritis is a source of osteoclast differentiation factor. Arthritis Rheum 43:250–258
41. **Tsuboi H, Udagawa N, Hashimoto J, Yoshikawa H, Takahashi N, Ochi T** 2005 Nurse-like cells from patients with rheumatoid arthritis support the survival of osteoclast precursors via macrophage colony-stimulating factor production Arthritis Rheum 52:3819–3828

Endocrinology **is published monthly by The Endocrine Society (http://www.endo-society.org), the foremost professional society serving the endocrine community.**